Int J Clin Exp Med 2017;10(4):6029-6041
www.ijcem.com /ISSN:1940-5901/IJCEM0044552

Original Article

MicroRNA-21 could promote the apoptosis of retinal neurons by down-regulating *PDCD4* in a rat model of diabetes mellitus

Ji Jin[1], Guo-Xu Xu[1], Ge-Hua Yu[2], Shu-Yang Bu[1]

[1]*Department of Ophthalmology, The Second Affiliated Hospital of Soochow University, Suzhou 215004, China;*
[2]*Department of Immunology, Immunology Laboratory, Soochow University, Suzhou 215004, China*

Received March 24, 2016; Accepted February 2, 2017; Epub April 15, 2017; Published April 30, 2017

Abstract: Objective: This study aimed to explore the effects of microRNA-21 (miR-21) on the apoptosis of retinal neurons by targeting programmed cell death 4 (PDCD4) in a rat model of diabetes mellitus (DM). Methods: Retinal neurons were isolated from SD rats and identified by fluorescence microscope. The retinal neurons were treated with a high concentration of glucose and divided into 5 groups: blank group (without any transfection), control group (transfected empty plasmid), anti-miR-21 group (transfected with anti-miR-21 inhibitor), sh-PDCD4 group (transfected with sh-PDCD4 plasmid) and anti-miR-21 + sh-PDCD4 group (transfected with anti-miR-21 inhibitor and sh-PDCD4 plasmid). Dual luciferase reporter assay was used to identify of the relationship between miR-21 and *PDCD4*. MTT assay and Hoechst33342 staining were applied for determining cell viability and apoptosis. The miR-21, PDCD4, apoptosis-related protein (Bcl-2 and Bax) expressions were detected by qRT-PCR assay and Western blotting. Fifty DM rats were equally and randomly assigned to 5 groups (10 rats in each group): normal, blank, control, anti-miR-21, and anti-miR-21 + sh-PDCD4 groups. All rats were executed 8 weeks after intravitreal injection with lentiviruses. HE staining and TUNEL staining were performed. Results: The luciferase reporter gene assay verified miR-21 could bind to the promoter sequence of PDCD4 3'UTR. Compared with the control and blank groups, cell viability was remarkably increased and the apoptosis rate was significantly decreased in the anti-miR-21 group, while the sh-PDCD group exhibited an opposite trend. The expressions of miR-21 and Bcl-2 were lower and the expressions of PDCD4 and Bax were higher in the anti-miR-21 group than those in the control and blank groups, while the expressions of miR-21 in sh-PDCD group had no obvious change, higher apoptosis rate and lower PDCD4 (all $P < 0.05$); however, opposite trends were observed in the anti-miR-21 + sh-PDCD4 group. In rat retinal tissues, the sh-PDCD4 group had markedly higher miR-21 expression and apoptosis rate but lower PDCD4 expression than the anti-miR-21 group (all $P < 0.05$), while the expressions of miR-21 in anti-miR-21 + sh-PDCD4 group had no significant difference, decreased PDCD4 and increased apoptosis rate (all $P < 0.05$). Conclusion: Our study provides evidence that miR-21 could promote the apoptosis of retinal neurons in DM rats by down-regulating *PDCD4*.

Keywords: MicroRNA-21, PDCD4, diabetes mellitus, retinal neuron, apoptosis

Introduction

Diabetic retinopathy (DR) is one of the most common and severe microvascular complications of diabetes mellitus (DM), and the leading cause of irreversible blindness characterized by abnormal retinal vasculature and neuronal dysfunction [1, 2]. More than 60% of adults with type II DM develop DR within 20 years of disease onset, causing 5% of blindness worldwide [3]. The main features of DR include endothelial proliferation, thickening of basement membrane, retinal ischemia and hypoxia, and neovascularization [4-6]. It has been found that the DR incidence was mainly induced by hyperglycemia and closely linked to hypertension and hyperlipidemia [7]. Currently, the treatments for DM are limited to tight control of blood glucose, blood pressure and blood lipid [8-10] with few drugs specifically targeting DM complications. As the population of DM patients is increasing dramatically, it has been extremely urgent to discover novel targets for the treatment and prevention of DM and its complications. Emerging evidence indicates that microRNAs (miRNAs) could play critical roles in the regulation of

diabetes and its complications via a series of closely related biological pathways [11, 12]. Besides, programmed cell death 4 (PDCD4) has been identified as a gene which is up-regulated during apoptosis [13].

MiRNAs are a group of endogenous, small, non-coding and single stranded RNA molecules, participating in almost all physiological and pathological processes *in vivo* (cell growth, development, proliferation, differentiation, apoptosis, etc.), mainly by inhibiting translation of mRNAs and degrading target mRNAs [14, 15]. Serum miRNAs have already been used as biomarkers for many diseases, including gliomas and gestational DM [16, 17]. Particularly, some miRNAs have been shown to play a vital role in the occurrence and development of DR [18-20], among which miR-21 has been reported to be a potential diagnostic biomarker for diabetic nephropathy [21] and exert important effects on cancer cell proliferation and apoptosis [22, 23]. Although miR-21 was independently expressed without being regulated from the overlapping promoters of protein-coding genes, due to its unique promoter, the activation protein 1 (AP-1) enhancer element is still able to regulate the expression of miR-21 in different cell signaling pathways [24]. Altering PDCD4 expression may therefore be a treatment option, particularly for tumors for which current treatment modalities are limited, such as neuroendocrine tumors [13]. To date, the role of miR-21 in DR has rarely been reported. Therefore, this study aims to investigate effects of miR-21 targeting *PDCD4* on retinal neuron apoptosis of DM rats, so as to further explore the functions of miR-21 in search of targets for the DR treatment.

Material and methods

Ethical statement

This study was performed in accordance with the approved animal protocols and guidelines established by Medicine Ethics Review Committee for animal experiments of the Second Affiliated Hospital of Soochow University for the use of laboratory animals.

Culture of retinal neuron

Neonatal SD rats (SIPPR-BK Laboratory Animal Co., Ltd., Shanghai, China), in 1~3 days after birth, were disinfected in 75% alcohol for 5 min and then the eyeballs were enucleated under sterile conditions in a clean bench and washed 3 times in an ice bath of phosphate buffered saline (PBS) containing 100 U/mL Penicillin and 100 μg/mL Streptomycin. The anterior segment tissue and vitreous body were removed from the annular incision (about 1 mm away from the corneoscleral limbus), and the retinas were separated from the pigment epithelium layer by blunt dissection, cut into segments with sizes of about 1 mm^2, and collected in centrifuge tubes. The retina fragments were treated with ten times the volume of 0.25% trypsin at 37°C for 15 min and the digestion was terminated by adding DMEM (Gibco BRL Co., Ltd., USA) containing 10% fetal bovine serum (FBS). Cells were aspirated by gently pipetting and single-cell suspensions were filtered with a 400-mesh stainless steel screen (Yuanxiang Medical Devices Co., Ltd. Shanghai, China), then centrifuged at 1000 rpm for 3 min. After the supernatant was discarded, the cells were suspended with DMEM containing 10% FBS. Cell density was adjusted to 1×10^6 cells/mL and then cells were inoculated in 6-well plates precoated with polylysine (Sigma, USA) before being cultured at 37°C in a 5% CO_2 atmosphere. The medium was replaced after 24 h by the maintenance medium containing 97.5% Neurobasal Medium, 2% B_{27} and 0.5% 200 mM/L L-Glutamine (Invitrogen, USA), and thereafter, refreshed every 2~3 days.

Establishment of high glucose models and grouping

The isolated retinal neurons were cultured for 3 days and then seeded in 24-well plates for establishment of high glucose models. The retinal neurons were divided into the control group and the experiment group in which the concentrations of glucose were 5, 20, 30 and 50 mmol/L respectively, and both groups were cultured for 24 h, 48 h and 72 h with cell morphology observed at each time point. The MTT assay was used for cell viability analysis so as to determine an appropriate glucose concentration for establishment of high glucose models.

Dual luciferase reporter assay

A miRNA target prediction software was used to predict the binding site between miR-21 and PDCD4 3'UTR. The synthesized promoter sequence of PDCD4 3'UTR containing the miR-

21 binding site was inserted into 5'-end at BglII site of pGL3 control vector (Promega Corp.) for construction of the PDCD4 3'UTR wild-type (WT) plasmid (named PDCD4 3'UTR-WT). The miR-21 binding site of PDCD4 3'UTR-WT was mutated to construct PDCD4 3'UTR mutant (MUT) plasmid (named PDCD4 3'UTR-MUT). Following the protocol of the plasmid extraction kit (Promega Corp.), cells were transfected with miR-21 mimics + *PDCD4*-WT (WT + mimics group), miR-21 mimics + *PDCD4*-MT (MT + mimics group), miR-21 NC + *PDCD4*-WT (WT + NC group) and miR-21 NC + *PDCD4*-MT (MT + NC group) respectively. The reporter gene vector used in the experiment was pcDNA3. I-luc which encodes firefly luciferases. For evaluation of the transfection efficiency, pRL-TK was co-transfected as an internal control, encoding Renilla luciferases. The fluorescent agent was preheated and parameters were set. After zero setting, 40 μL LARII and 40 μL STOP&Glo Reagent were added into fluorescent tubes and then placed into a fluorometer with corresponding fluorescence values recorded.

Cell grouping and transfection

The retinal neurons treated with a high concentration of glucose were divided into 5 groups, control group (transfected empty plasmid), anti-miR-21 group (transfected with anti-miR-21 inhibitor), anti-miR-21 + sh-PDCD4 group (transfected with anti-miR-21 inhibitor, sh-PDCD4 (transfected with sh-PDCD4 plasmid) and sh-PDCD4 plasmid) and blank group (without any transfection). There plasmid vectors were constructed by Shanghai Genechem Co. Ltd. Cells in each group were digested with trypsin and then seeded in 6-well plate with a certain cell density. After 6 hr, cells were attached and each well was treated with 1 mL of virus stock solution (Invitrogen, USA) diluted by culture medium containing 5 μg/mL polybrene. The cells were then cultured in an incubator for 120 hrs before subsequent experiments.

MTT assay

Cell suspensions were diluted in a certain proportion and seeded in a polylysine-coated 96-well plate (Sigma, USA) at a density of 5×10^4 cells/well, which were then cultured in an incubator until cells were grown to 80% confluence. The cells were grouped as above, with 6 wells in each group, and cultured for 24 h, 48 h and 72 h, respectively. After the medium was removed, the plate was washed by the serum-free medium for 3 times, treated with 20 μL of MTT (Sigma, USA) and incubated at 37°C for 4 hrs. MTT was then discarded and 150 μL dimethyl sulfoxide (Sigma, USA) was added to each well. The plate was placed on a shaker for 10 min and the optical density (OD) value of each well was determined at 490 nm on a microplate reader. Each sample was measured in triplicate with the mean value calculated. Cell viability = $(OD_{\text{experiment group}} - OD_{\text{blank group}})/OD_{\text{blank group}}$.

Hoechst33342 staining

The retinal neurons in the above mentioned groups were seeded in a polylysine-coated 6-well plate. Grown to 80% confluence, cells in the control group and the glucose treatment groups (5, 20, 30 and 50 mmol/L, respectively) were processed and further cultured for 48 h before Hoechst33342 staining. Following the protocol of Hoechst33342 staining (Fan Bo Biochemical Co., Ltd., Beijing, China), the medium was removed from slides which were then washed by PBS for 2 times and fixed in 4% paraformaldehyde for about 30 min. Washed in PBS for 2 times, each slide was stained with 0.5 mL Hoechst33342 for 30 min before being washed by PBS for 3 times. The samples were then observed under a fluorescence microscope and the cells in 3 random fields were selected and scored with at least 500 cells counted. Apoptosis rate = the number of apoptotic cells/the total number of cells.

Quantitative real-time polymerase chain reaction (qRT-PCR)

According to the kit's instruction (QIAGEN, Valencia, CA), total RNA was extracted from retinal tissues and retinal neurons in each group. After the OD260/280 value of each RNA sample was determined by UV spectrophotometer with corresponding concentration of RNA calculated, samples were stored at -80°C and then reversely transcribed, following the manufacturer's instruction (QIAGEN, Valencia, CA). Based on gene sequences in the Genbank databases and miRBase databases, specific primers with stem-loop structures and PCR primers were correspondingly designed for reverse transcription and PCR amplification using Primer 5.0 software. The sequences were

Table 1. Primer sequences for quantitative real-time polymerase chain reaction (qRT-PCR)

Gene	Sequence
miR-21	F: 5'-ACACTCCAGCTGGGTAGCTTATCAGACTGA-3'
	R: 5'-CTCAACTGGTGTCGTGGAGTCGGCAATTCAGTTGAGTCAACATC-3'
PDCD4	F: 5'-GCTGAACATTGCCTTAAGGA-3'
	R: 5'-CCCTTGAAGGACAAAGATCT-3'
Bcl-2	F: 5'-CAGATGCACCTGACGCCCTT-3'
	R: 5'-AGGTCCTATTGCCTCCGACCC-3'
Bax	F: 5'-TGGCAGCTGACATGTTTTCTGAC-3'
	R: 5'-TCTGGTCCCACAACCCCTGC-3'
U6	F: 5'-CTCGCTTCGGCAGCACA-3'
	R: 5'-CTCGCTTCGGCAGCACA-3'
β-actin	F: 5'-GCCATCCTGCGTCTG-3'
	R: 5'-GGGGCATCGGAACCGCT-3'

F, Forward; R, Reverse.

showed in **Table 1**. The primers were designed by Sangon Biotech (Shanghai) Co. Ltd. The volume of the qRT-PCR system was 20 μL (SYBR PremixExTaq 10 μL, Forward Primer 0.4 μL, Reverse Primer 0.4 μL, ROX Reference Dye II 0.4 μL, DNA template 2 μL and dH_2O 6.8 μL) and reaction conditions were 95°C for 30 s, 95°C for 5 s, 60°C for 30 s, followed by 40 cycles of amplification. With U6/β-actin as the internal control, the melting curves were applied to evaluate the reliability of PCR results. The threshold cycle (f'fCt) values were set (the inflection points of amplification curves) and the relative expression levels of target gene were calculated based on the $2^{-\Delta\Delta Ct}$ method [25].

Western blotting

Proteins were extracted from the retinal tissues and neurons in each group and corresponding concentrations were determined according to the instruction of the BCA kit (Beyotime Co., Ltd, Beijing, China). Extracted proteins were mixed with the loading buffer and then heated at 95°C for 10 min. The mixture (30 μg/well) was loaded onto a 10% polyacrylamide gel (Beyotime Co., Ltd, Beijing, China), underwent electrophoresis under the voltage from 80 V to 120 V, and were subsequently transferred to a polyvinylidene fluoride (PVDF) membrane (100 mV for 45~70 min) that was blocked with 5% BSA for 1 hr and incubated with PDCD4 primary antibodies (1:1000, Bioworld Technology, Inc., USA), Bax (mouse monoclonal, 1:200 dilution; Santa Cruz, USA), Bcl-2 (mouse monoclonal, 1:500 dilution; Santa Cruz, USA) at 4°C overnight. Washed by TBST (3 times/5 min), the membrane was incubated with second antibodies for 1 hr and then washed by TBST (3 times/5 min) before chemiluminescence detection. With β-actin as the internal reference, the Bio-Rad Gel Doc EZ system was used to visualize the protein bands and grey value analysis for target bands was performed using the Image J software.

Establishment of animal models and grouping

Fifty male SD rats (body weights of 180 ± 20 g) were purchased from Shanghai SIPPR-BK Laboratory Animal Co., Ltd. and housed in a specific pathogen-free (SPF) animal center of the Second Affiliated Hospital of Soochow University. The temperature was maintained at 23~25°C, the humidity was 60% and rats were fed on a free diet. For the establishment of DM rat models, at the 48th hrs after 40 SD rats were injected intraperitoneally with 1% Streptozocin (STZ, purchased from Sigma, USA) at a dose of 60 mg/kg, blood glucose levels were determined from the tail vein and the rats with blood glucose levels over 16.7 mmol/L were screened out for subsequent experiments while those with lower blood glucose levels were removed. The remaining 10 rats without the STZ treatment were categorized into the normal group. Theses rats were equally and randomly assigned to 5 groups (10 rats in each group): normal control (healthy normal rats), blank (DM rats), negative control (DM rats without any transfection), anti-miR-21 (DM rats transfected with anti-miR-21 plasmid), anti-miR-21 + sh-PDCD4 (DM rats transfected with anti-miR-21 and sh-PDCD4 plasmids) groups. All plasmid vectors were constructed by Shanghai Genechem Co., Ltd. and packaged into lentiviruses with a titer of 10^9/mL.

Intravitreal injection with lentiviruses

In a clean bench, 2 μL of solution for enhancement of virus infection (Genechem Co., Ltd,

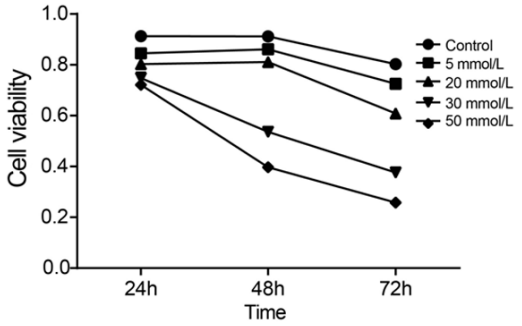

Figure 1. Cell viability of retinal neurons treated with different concentrations of glucose in each group at different time points (24 h, 48 h and 72 h).

Shanghai, China) was mixed with 200 μL virus stock solution in each group. Rats were anesthetized with 10% chloral hydrate, disinfected by 2% iodophor and treated with compound tropicamide eye drops to dilate the pupils before the injection. A needle was inserted through the vitreous body from the corneal limbus, and lentiviruses were slowly injected by a micro injector, under a dissecting microscope. After the needle was pulled out, the injected eye was oppressed for 1 min. The dose of lentivirus was 10 μL for each eye, and 10 μL negative virus solution was injected into every rat in the control group.

Preparation of retinal paraffin sections

Rats after 8-week treatment were anesthetized by 10% chloral hydrate and then dissected with their hearts exposed. The left ventricular apexes were cut, subsequently inserted by the needle of the infusion pump, with the other end of the infusion pump immersed in saline. The right atrial appendages were rapidly cut, of which blood flowed out, and the infusion pump was immediately turned on. The hearts were washed by saline until the effluent became clear and then slowly infused with 4% paraformaldehyde until the limbs of rats became stiff. The eyeballs were taken, fixed with 4% paraformaldehyde for 12 hrs and washed by running water for 24 h. The ocular walls were cut at the posterior of dentate margin, from which anterior segments and vitreous bodies were taken. The remaining ocular walls were dehydrated with an ethanol series, cleared by xylene and fully embedded in paraffin from which 8 μL paraffin sections were taken.

HE staining

The sections were treated with 100% xylene I for 10 min and 100% xylene II for 10 min. Gradient dehydration: the section was treated with an ethanol series from high concentrations to low concentrations (5 min each time) and then immersed in distilled water for 3 min. Hansen's hematoxylin staining: the cell nucleus was stained violet after 7~10 min. Differentiation: the section was treated with saline and ethanol (1:1), then immersed in ammonia water and eventually stained dark blue. Hematoxylin and eosin staining: the section, except the cytoplasm, was stained for 6 min. Dehydration: an ethanol series from low concentrations to high concentrations (5 concentrations, 5 min each time). Cleared by 100% xylene I for 5 min and 100% xylene II for 5 min, the sections were sealed with neutral gum.

TUNEL staining

The samples were analyzed with TUNEL kit (Beyotime Co., Ltd, Beijing, China) and evaluated by the apoptosis index (AI). The prepared paraffin sections were treated with certain concentrations and doses of protease K, incubated at 37°C for 30 min, washed by PBS for 5 times, immersed in 0.1% Triton X-100 buffer on a shaker for 15 min and washed by PBST for 5 times later. Following the manufacturer's instructions, the incubation buffer was prepared and added to retinal sections which were incubated in a water bath at 37°C for 60 min and then washed by PBST for 5 times. Treated with corresponding antibodies, the tissue sections were incubated at 37°C for 30 min in the dark, followed by POD addition and DAB staining. The slides were washed by tap water, cleared by xylene, hydrated in an ethanol series from 100% to 60% (5 min for each concentration), sealed with neutral gum, dried for 12 hrs and eventually observed under a light microscope. Five fields per sample were taken with a light microscope at 400 × magnification and the numbers of positive cells and retinal neurons were calculated. AI = the number of positive cells/the total number of retinal neurons.

Statistical analysis

SPSS18.0 software was used for statistical analysis and measure data were expressed

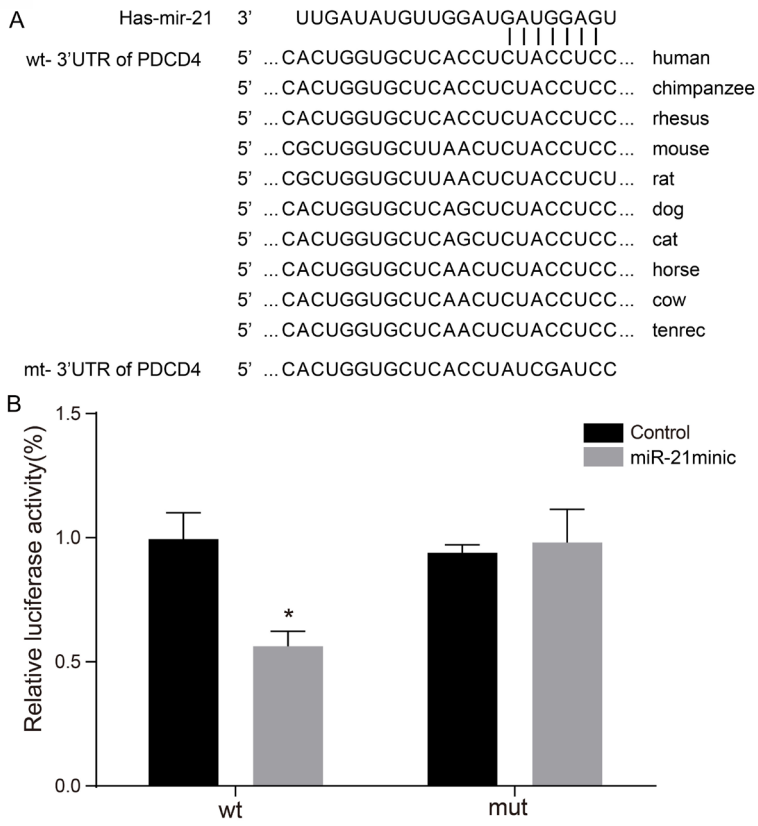

Figure 2. The relative luciferase activities of cells co-transfected with PDCD4 3'UTR and miR-21 mimics. Note: A. Comparison of miR-21 and PDCD4 3'UTR sequences; B. The relative luciferase activities of cells transfected with PDCD4 3'UTR, miR-21 mimics and miR-21 NC. *, $P < 0.05$, compared with the corresponding miR-21 NC group.

by $\bar{x} \pm s$. The two groups in normal distribution were compared using the *t* test and the multiple groups were compared using one-way analysis of variance (One-Way ANOVA). Bonferroni's post-hoc analysis was performed after significance was determined by ANOVA. Count data was detected by chi-square test and expressed as percentage or rate. Correlation analysis was tested with Pearson correlation analysis. $P < 0.05$ showed statistical difference.

Results

Determination of the glucose concentration and establishment of high glucose model

The MTT assay showed that retinal neurons in the control group had no significant difference over time points ($P > 0.05$). In the glucose groups, it was shown that the cell viability of retinal neurons decreased substantially after treated with 30 mmol/L glucose for 48 h. Thus, high glucose models were established under the treatment of 30 mmol/L glucose for 48 h (**Figure 1**).

MiR-21 targeting PDCD4

Prediction of miR-21 targeting *PDCD4* was accomplished by the online software Targetscan (http://www.targetscan.org/) and the binding sites between the 3' untranslated region (3'UTR) of PDCD4 and miR-21 was highly conserved in rats (**Figure 2A**). The luciferase reporter gene assay showed that the relative luciferase activities of cells co-transfected with PDCD4 3'UTR-WT and miR-21 mimics were significantly lower than those in the corresponding miR-21 NC group without miR-21 transfection ($P < 0.01$) whereas no changes in the relative luciferase activities was observed in the PDCD4 3'UTR-MUT + miR-21 mimics group and the corresponding miR-21 NC group (**Figure 2B**). Experiment results were consistent with the prediction of bioinformatics, which verified miR-21 could bind to the promoter sequence of PDCD4 3'UTR and implied miR-21 could inhibit PDCD4 by targeting its mRNA.

Effects of miR-21 on the viability and apoptosis of retinal neurons

Compared with the control group and the blank group, the cell viability in the anti-miR-21 group saw a marked increase, while an opposite trend was observed in the anti-miR-21 + sh-PDCD4 group and sh-PDCD4 group (all $P < 0.05$) (**Figure 3A**). Hoechst33342 staining was applied for assessment of apoptosis at 48 h (**Figure 4**). Many nuclei in the control group and the blank group showed various apoptotic morphological characteristics, such as chromatin condensation, pyknosis, karyorrhexis and chromatin margination. Similarly, apoptotic morphological characteristics, including chromatin condensation and karyorrhexis, could also be observed

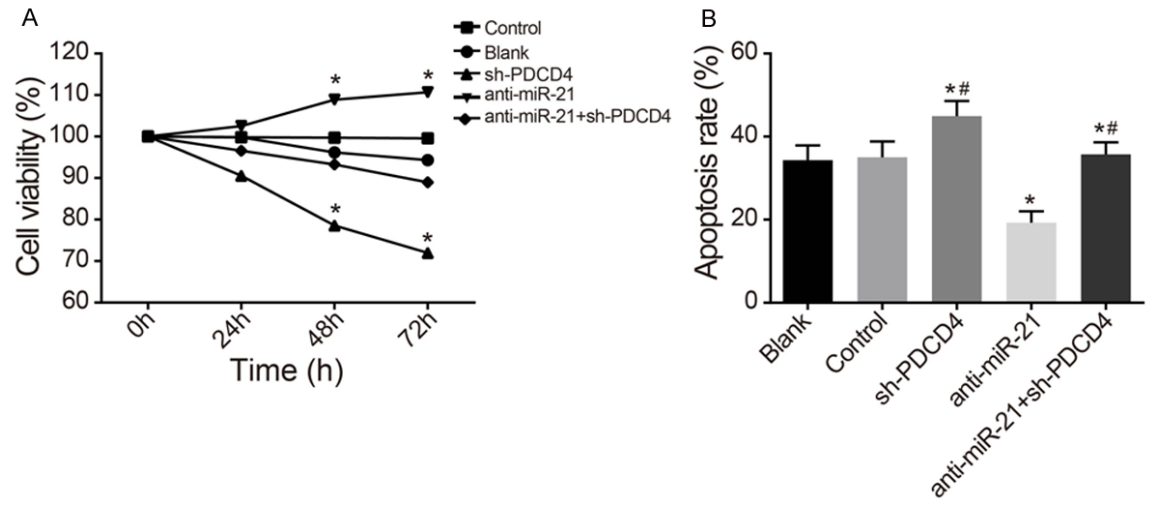

Figure 3. Effects of miR-21 targeting PDCD4 on the viability and apoptosis of retinal neurons. Note: A: Viability at different time point by MTT assay, *, $P < 0.05$, compared with the control group and the blank group; B: Apoptosis of each group in 48 h by Hoechst33342 staining, *, $P < 0.05$, compared with the control group and the blank group; # $P < 0.05$, compared with the anti-miR-21 group.

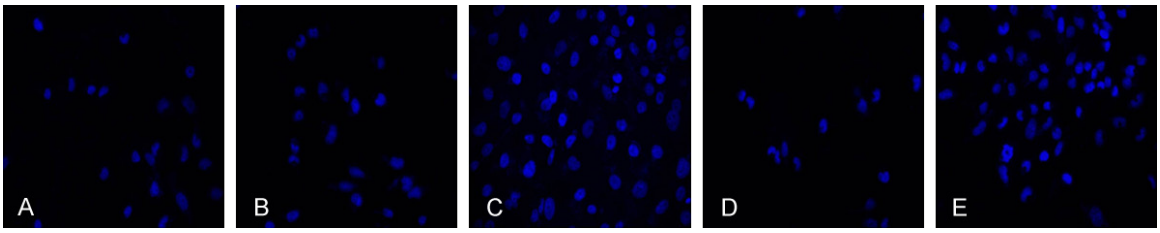

Figure 4. Hoechst33342 staining. Note: A: Blank group; B: Control group; C: sh-PDCD4 group; D: Anti-miR-21 group; E: Anti-miR-21 + sh-PDCD4 group.

in a larger number of nuclei in the anti-miR-21 + sh-PDCD4 group, in contrast to nuclei in the anti-miR-21 group which were evenly stained light blue. There existed significant difference among groups on apoptosis rate, in which the apoptosis rate decreased substantially in the anti-miR-21 group but increased significantly in the sh-PDCD4 group when compared with those in the control group and the blank group (**Figure 3B**).

Expression of miR-21, PDCD4 and apoptosis-related proteins in retinal neurons

The qRT-PCR was applied to determine expression of miR-21, PDCD4 mRNA and the mRNA expressions of apoptosis-related proteins both in the normal retinal neuron group and the high glucose group which was treated with 30 mmol/L glucose for 48 h. Compared with the blank and control groups, the expressions of miR-21 and Bax were lower and the expressions of PDCD4 and Bacl-2 were higher in the anti-miR-21 group; however, in the anti-miR-21 + sh-PDCD4 group, the expressions of miR-21 decreased markedly and other factors had no obvious change. The expressions of miR-21 in sh-PDCD4 group had no significant difference in comparison to control group and blank group, while the expressions of PDCD4 and Bacl-2 were lower and Bax were higher in sh-PDCD4 group (all $P < 0.05$) (**Figure 5**). Pearson correlation analysis indicated that the expression level of miR-21 was negatively correlated with that of PDCD4 mRNA ($r = -0.54$, $P < 0.05$).

Expression of miR-21 and PDCD4 in retinal tissues

The negative control, blank, sh-PDCD4 and anti-miR-21 + sh-PDCD4 groups had significantly higher miR-21 mRNA expressions but

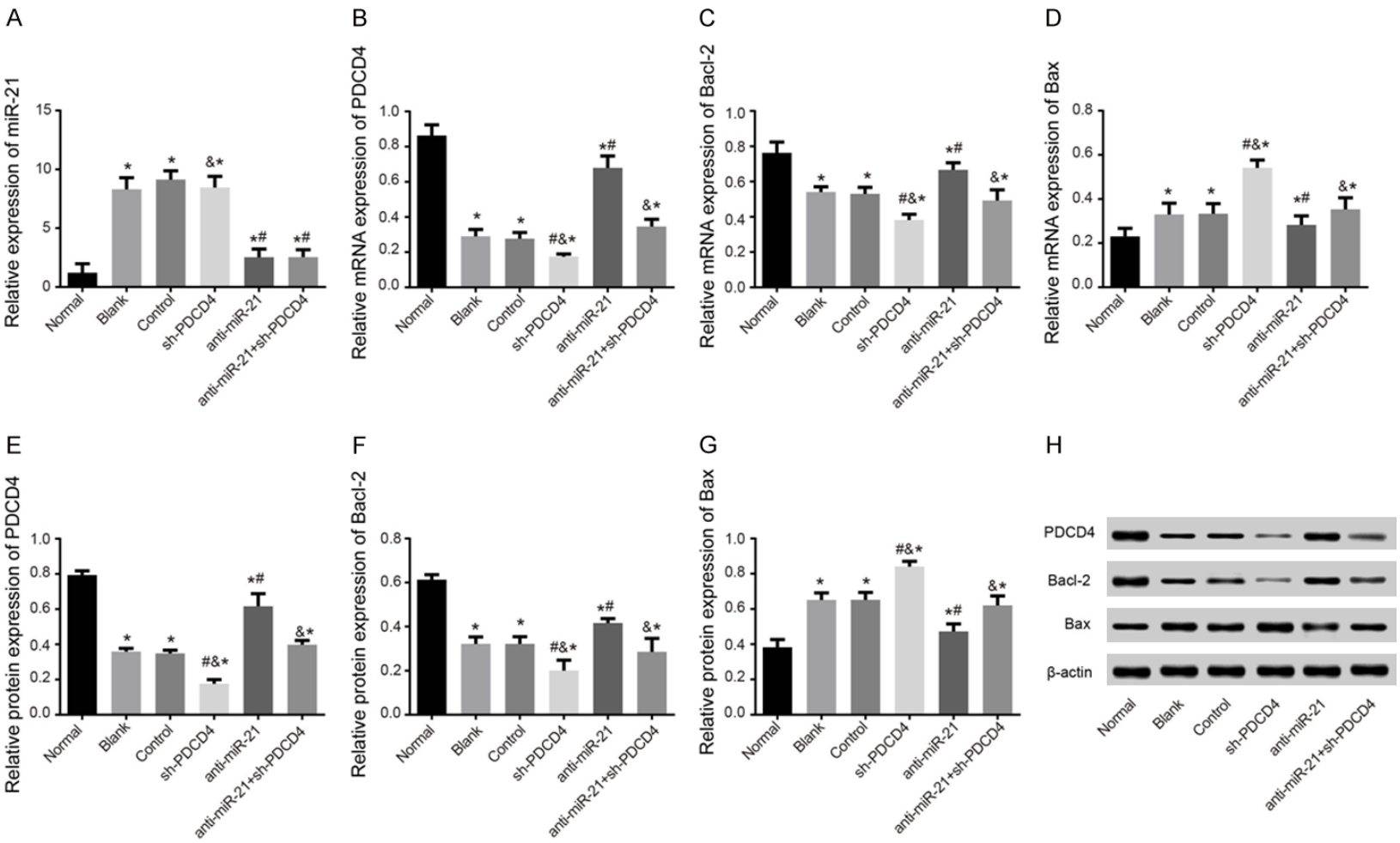

Figure 5. Expression of miR-21, PDCD4 and apoptosis-related proteins (Bcl-2 and Bax) in retinal neurons. Note: A. The relative expression of miR-21 in each group; B. The mRNA expression of PDCD4 in each group; C. The mRNA expression of Bcl-2 in each group; D. The mRNA expression of Bax in each group; E. The protein expression of PDCD4 in each group; F. The protein expression of Bcl-2 in each group; G. The protein expression of Bax in each group; H. Western blots of the protein expression of PDCD4 and apoptosis-related proteins (Bcl-2 and Bax) in each group. *, $P < 0.05$, compared with the normal group; #, $P < 0.05$, compared with the control and the blank group; &, $P < 0.05$, compared with the anti-miR-21 group.

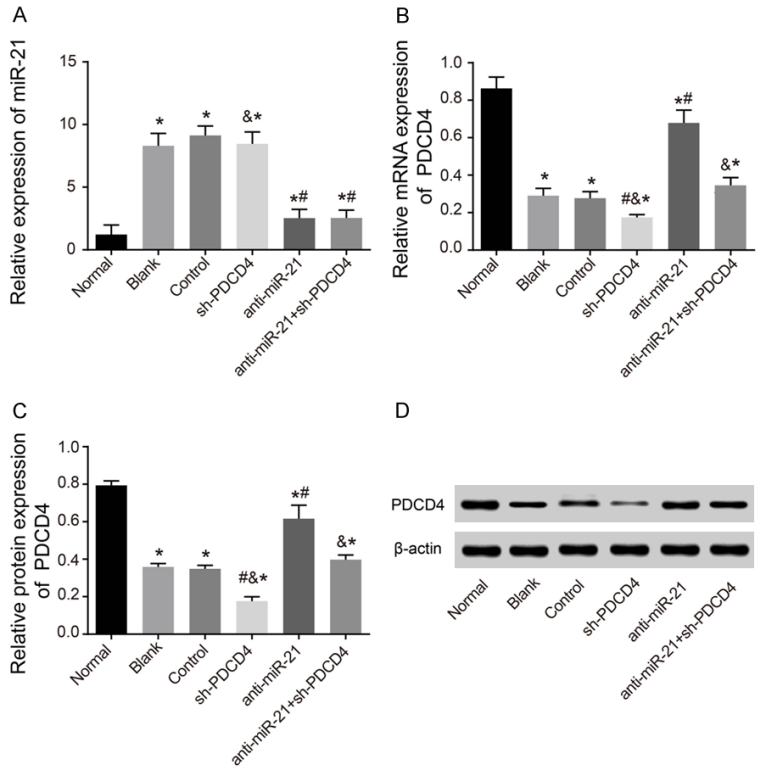

Figure 6. Expression of miR-21 and PDCD4 in retinal tissues. Note: A. The relative expression of miR-21 in each group; B. The mRNA expressions of PDCD4 and apoptosis-related proteins in each group; C. Relative protein expressions of PDCD4; D. Western blotting bands of PDCD4. *, $P < 0.05$, compared with the normal group; #, $P < 0.05$, compared with the control and the blank group; &, $P < 0.05$, compared with the anti-miR-21 group.

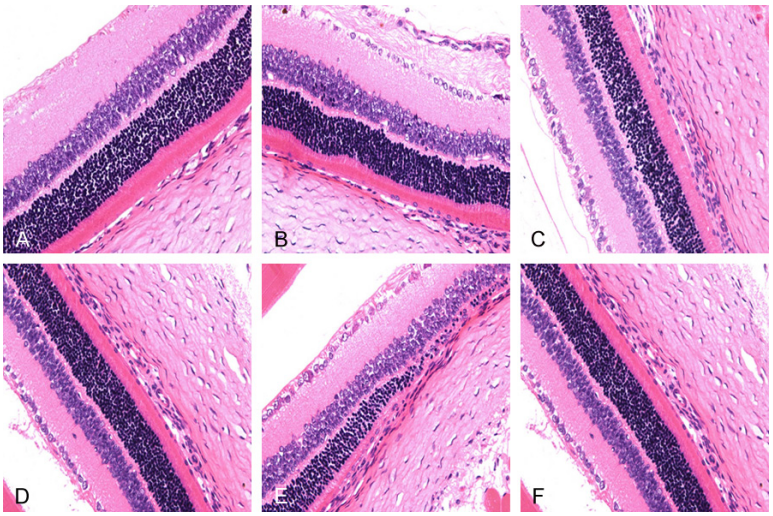

Figure 7. HE staining of retinal neural cells. Note: A: Normal group; B: Blank group; C: Control group; D: sh-PDCD4 group; E: Anti-miR-21 group; F: Anti-miR-21 + sh-PDCD4 group.

markedly lower PDCD4 mRNA and PDCD4 protein expressions than the normal control group (all $P < 0.05$). The expressions of miR-21 mRNA in sh-PDCD4 group had no significant change (all $P > 0.05$), while the protein expressions of PDCD4 mRNA and PDCD4 decreased markedly (all $P < 0.05$). When compared with the control group and the blank group, the anti-miR-21 + sh-PDCD4 group experienced a substantial decrease in the expression level of miR-21 mRNA but no significant difference both in expression levels of PDCD4 mRNA and PDCD4 expressions (all $P < 0.05$). In comparison to anti-miR-21 group, the expressions of miR-21 mRNA in sh-PDCD4 group increased (all $P > 0.05$), while the protein expressions of PDCD4 mRNA and PDCD4 declined significantly. The expression level of miR-21 mRNA was not significantly differenced, but PDCD4 mRNA and PDCD4 expression declined substantially in the anti-miR-21 + sh-PDCD4 group against the anti-miR-21 group (all $P < 0.05$) (**Figure 6**).

HE staining of retinal tissues of rats in each group

HE staining showed that, in normal group, few apoptotic cells appeared in ganglion cell layer, and there were no apoptotic cells in inner and outer nuclear layer (**Figure 7A**); in anti-miR-21 group, apoptotic cells mainly appeared in ganglion cell layer and inner nuclear layer, no apoptotic cells in outer nuclear layer (**Figure 7E**); in blank group and control group, many apoptotic cells appeared in ganglion cell layer and inner nuclear layer, and few apoptotic cells in outer nuclear layer (**Figure 7B**, **7C**); in sh-PDCD4 group and anti-miR-21 + sh-PDCD4 group, there were

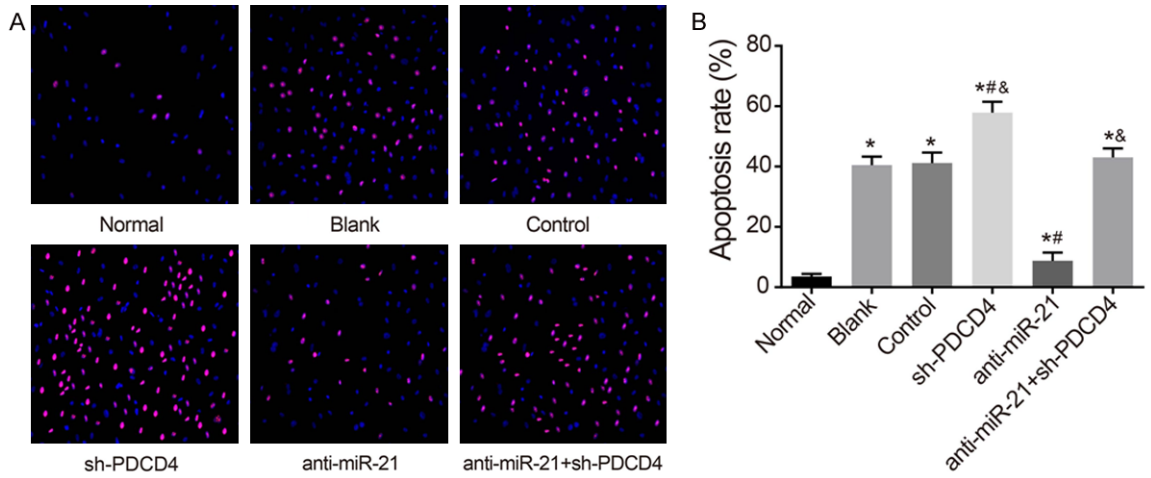

Figure 8. TUNEL staining for determination of apoptosis rates of retinal neurons in each group. Note: A. Fluorescence-based TUNEL staining for apoptosis rates of retinal neurons in each group; B. Comparison of the apoptosis rates of retinal neurons in each group. *, $P < 0.05$, compared with normal group; #, $P < 0.05$, compared with control and blank group; &, compared with anti-miR-21 group.

more apoptotic cells appeared in ganglion cell layer, inner and outer nuclear layer than blank and control group (**Figure 7D**, **7F**).

Cell apoptosis in retinal tissues of rats in each group

TUNEL staining showed that the control, blank, sh-PDCD4 group and anti-miR-21 + sh-PDCD4 groups exhibited significant an increase in the apoptotic rate in comparison to the normal group (all $P < 0.05$). The anti-miR-21 group presented substantially fewer apoptotic cells while the sh-PDCD4 group had significantly increased apoptotic cells, compared with the control group and the blank group (both $P < 0.05$) (**Figure 8**).

Discussion

In this study, retinal neurons isolated from SD rats were selected as the research objects and treated with 30 mmol/L glucose for 48 h for establishment of hyperglycemia models, which aimed to explore effects of miR-21 targeting programmed cell death 4 (PDCD4) on the apoptosis of retinal neurons in DM rats. Our results found that miR-21 could promote the apoptosis of retinal neurons in DM rats through targeting PDCD4 expression, which might provide a promising therapeutic target in the DR treatment.

This study firstly determined miR-21 and PDCD4 expression in retinal neurons, showing that the high glucose group experienced a significant increase in miR-21 expression and correspondingly, substantial declines in PDCD4 mRNA and protein expression when compared to the normal group, which is consistent with Dey's finding that miR-21 expression was markedly elevated in renal cortex of DM rats [26]. Regarding retinal neurons in the high glucose group, the underlying mechanisms of DR might include: the expression of intracellular adhesion molecules is increased, accompanied by peroxide generation [4]; activation of PKC and NF-κB induces symptoms similar to retinal ischemia and hypoxia [27, 28]; activation of c-Rel and p65 in the NF-κB family stimulates the miR-21 promoter and subsequently up-regulates the miR-21 expression [29]. Moreover, it has been reported that Smad3 promotes TGF-β-induced miR-21 expression via binding to the promoter region of miR-21 under the hyperglycemia condition [30]. On the other hand, PDCD4, acting as an important anti-apoptotic factor, was down-regulated in the high glucose group, probably because thickening of retinal capillary basement membrane increased vascular permeability, making small blood vessels more likely to deform and leak.

Further study has demonstrated the targeted inhibition of miR-21 on *PDCD4*, and their negative correlation has been proven [31]. Similarly, it was reported that *PDCD4* is a target gene of miRNA-21 and participates in miRNA-21-regulated apoptosis in urothelial carcinoma [32],

implying that similar relationship between *PDCD4* and miRNA-21 might also exist in retinal neurons. Therefore, changes of miRNA-21 and PDCD4 might reflect the extent of apoptosis under different concentrations of insulin, but the targeted inhibition of miR-21 on *PDCD4* might be regulated by various mechanisms and involved in several self-regulating loops [33, 34].

In the apoptosis assay, it has been proved that apoptosis of retinal neurons in DM rates were associated with overexpression of miR-21 and down-regulation of PDCD4, similar to the conclusion in another report that knockdown of renal miR-21 improved renal fibrosis [35]. It has been verified that down-regulation of miR-21 could restore Smad7 levels, suppress hyperglycemia-activated TGF-β and NF-κB signaling pathways and reduce apoptosis [36]. On the other hand, decreased cell viability and increased apoptosis rates in the anti-miR-21 + sh-PDCD4 group illustrated that down-regulating PDCD4 expression attenuated its inhibition effect on apoptosis and promote apoptosis. In Sachiko's study, PDCD4 has been reported to exert similar effects on apoptosis of hepatocellular carcinoma cells [37], probably due to PDCD4 down-regulation and subsequent angiopoietin up-regulation [38].

In conclusion, this is the first study to investigate effects of miR-21 targeting *PDCD4* on the apoptosis of retinal neurons in DM rats Our results demonstrated a negative correlation between miR-21 and PDCD4 in retinal neurons and DM rats tissues, and verified that regulation of miR-21 could promote the apoptosis of retinal neurons in DM rats through targeting PDCD4 expression, which provided a potential and promising target for the DR treatment. Nevertheless, due to complex nature of this multi-factorial disease, further studies are still required to unravel its specific regulation and occurrence mechanisms.

Acknowledgements

We would like to acknowledge the helpful comments on this paper received from our reviewers.

Disclosure of conflict of interest

None.

Address correspondence to: Dr. Shu-Yang Bu, Department of Ophthalmology, The Second Affiliated Hospital of Soochow University, No. 181 Sanxiang Road, Suzhou 215004, China. Tel: +86-512-6828-2030; Fax: +86-512-68282030; E-mail: Soochow_bsy215@126.com

References

[1] Gao L, Xin Z, Yuan MX, Cao X, Feng JP, Shi J, Zhu XR and Yang JK. High prevalence of diabetic retinopathy in diabetic patients concomitant with metabolic syndrome. PLoS One 2016; 11: e0145293.

[2] Kern TS. Interrelationships between the retinal neuroglia and vasculature in diabetes. Diabetes Metab J 2014; 38: 163-170.

[3] Zhong X, Du Y, Lei Y, Liu N, Guo Y and Pan T. Effects of vitamin D receptor gene polymorphism and clinical characteristics on risk of diabetic retinopathy in Han Chinese type 2 diabetes patients. Gene 2015; 566: 212-216.

[4] Kowluru RA, Kowluru A, Mishra M and Kumar B. Oxidative stress and epigenetic modifications in the pathogenesis of diabetic retinopathy. Prog Retin Eye Res 2015; 48: 40-61.

[5] Diabetic retinopathy assessment: towards an automated system. Biomedical Signal Processing and Control 2016; 24: 72-82.

[6] Correction of diabetes-induced endothelial progenitor dysfunction to promote retinal vascular repair. Advances in Predictive, Preventive and Personalised Medicine 2013; 3: 147-174.

[7] Hendrick AM, Gibson MV and Kulshreshtha A. Diabetic retinopathy. Prim Care 2015; 42: 451-464.

[8] Do DV, Wang X, Vedula SS, Marrone M, Sleilati G, Hawkins BS and Frank RN. Blood pressure control for diabetic retinopathy. Sao Paulo Med J 2015; 133: 278-279.

[9] Zhu CH, Zhang SS, Kong Y, Bi YF, Wang L and Zhang Q. Effects of intensive control of blood glucose and blood pressure on microvascular complications in patients with type II diabetes mellitus. Int J Ophthalmol 2013; 6: 141-145.

[10] Lim LS and Wong TY. Lipids and diabetic retinopathy. Expert Opin Biol Ther 2012; 12: 93-105.

[11] Agrawal S and Chaqour B. MicroRNA signature and function in retinal neovascularization. World J Biol Chem 2014; 5: 1-11.

[12] Farr RJ, Januszewski AS, Joglekar MV, Liang H, McAulley AK, Hewitt AW, Thomas HE, Loudovaris T, Kay TW, Jenkins A and Hardikar AA. A comparative analysis of high-throughput platforms for validation of a circulating microRNA signature in diabetic retinopathy. Sci Rep 2015; 5: 10375.

[13] Lankat-Buttgereit B, Muller S, Schmidt H, Parhofer KG, Gress TM, and Goke R. Knockdown of Pdcd4 results in induction of proprotein convertase 1/3 and potent secretion of chromogranin A and secretogranin II in a neuroendocrine cell line. Biol Cell 2008; 100: 703-715.
[14] Yuan Z, Ding S, Yan M, Zhu X, Liu L, Tan S, Jin Y, Sun Y, Li Y and Huang T. Variability of miRNA expression during the differentiation of human embryonic stem cells into retinal pigment epithelial cells. Gene 2015; 569: 239-249.
[15] Desvignes T, Batzel P, Berezikov E, Eilbeck K, Eppig JT, McAndrews MS, Singer A and Postlethwait JH. miRNA nomenclature: a view incorporating genetic origins, biosynthetic pathways, and sequence variants. Trends Genet 2015; 31: 613-626.
[16] Wang Y, Wang X, Zhang J, Sun G, Luo H, Kang C, Pu P, Jiang T, Liu N and You Y. MicroRNAs involved in the EGFR/PTEN/AKT pathway in gliomas. J Neurooncol 2012; 106: 217-224.
[17] Zhao C, Dong J, Jiang T, Shi Z, Yu B, Zhu Y, Chen D, Xu J, Huo R, Dai J, Xia Y, Pan S, Hu Z and Sha J. Early second-trimester serum miRNA profiling predicts gestational diabetes mellitus. PLoS One 2011; 6: e23925.
[18] miR-200b regulates endothelial to mesenchymal transition in diabetic retinopathy. Canadian Journal of Diabetes 2014; 38: S61.
[19] Mastropasqua R, Toto L, Cipollone F, Santovito D, Carpineto P and Mastropasqua L. Role of microRNAs in the modulation of diabetic retinopathy. Prog Retin Eye Res 2014; 43: 92-107.
[20] Zhang T, Li L, Shang Q, Lv C, Wang C and Su B. Circulating miR-126 is a potential biomarker to predict the onset of type 2 diabetes mellitus in susceptible individuals. Biochem Biophys Res Commun 2015; 463: 60-63.
[21] Wang J, Duan L, Tian L, Liu J, Wang S, Gao Y and Yang J. Serum miR-21 may be a potential diagnostic biomarker for diabetic nephropathy. Exp Clin Endocrinol Diabetes 2016; 124: 417-23.
[22] Wang Z, Yang H and Ren L. MiR-21 promoted proliferation and migration in hepatocellular carcinoma through negative regulation of Navigator-3. Biochem Biophys Res Commun 2015; 464: 1228-1234.
[23] Zhou S, Zhang S, Wang Y, Yi S, Zhao L, Tang X, Yu B, Gu X and Ding F. MiR-21 and miR-222 inhibit apoptosis of adult dorsal root ganglion neurons by repressing TIMP3 following sciatic nerve injury. Neurosci Lett 2015; 586: 43-49.
[24] Zhu Q, Wang Z, Hu Y, Li J, Li X, Zhou L and Huang Y. miR-21 promotes migration and invasion by the miR-21-PDCD4-AP-1 feedback loop in human hepatocellular carcinoma. Oncol Rep 2012; 27: 1660-1668.
[25] Ruan Q, Wang T, Kameswaran V, Wei Q, Johnson DS, Matschinsky F, Shi W and Chen YH. The microRNA-21-PDCD4 axis prevents type 1 diabetes by blocking pancreatic beta cell death. Proc Natl Acad Sci U S A 2011; 108: 12030-12035.
[26] Dey N, Das F, Mariappan MM, Mandal CC, Ghosh-Choudhury N, Kasinath BS and Choudhury GG. MicroRNA-21 orchestrates high glucose-induced signals to TOR complex 1, resulting in renal cell pathology in diabetes. J Biol Chem 2011; 286: 25586-25603.
[27] Ganesh Yerra V, Negi G, Sharma SS and Kumar A. Potential therapeutic effects of the simultaneous targeting of the Nrf2 and NF-kappaB pathways in diabetic neuropathy. Redox Biol 2013; 1: 394-397.
[28] Madhyastha R, Madhyastha H, Pengjam Y, Nakajima Y, Omura S and Maruyama M. NF-kappaB activation is essential for miR-21 induction by TGFbeta1 in high glucose conditions. Biochem Biophys Res Commun 2014; 451: 615-621.
[29] Li Y, Dai D, Lu Q, Fei M, Li M and Wu X. Sirt2 suppresses glioma cell growth through targeting NF-kappaB-miR-21 axis. Biochem Biophys Res Commun 2013; 441: 661-667.
[30] Liang H, Zhang C, Ban T, Liu Y, Mei L, Piao X, Zhao D, Lu Y, Chu W and Yang B. A novel reciprocal loop between microRNA-21 and TGFbetaRIII is involved in cardiac fibrosis. Int J Biochem Cell Biol 2012; 44: 2152-2160.
[31] Wang G, Wang JJ, Tang HM and To SS. Targeting strategies on miRNA-21 and PDCD4 for glioblastoma. Arch Biochem Biophys 2015; 580: 64-74.
[32] Fischer N, Goke F, Splittstosser V, Lankat-Buttgereit B, Muller SC and Ellinger J. Expression of programmed cell death protein 4 (PDCD4) and miR-21 in urothelial carcinoma. Biochem Biophys Res Commun 2012; 417: 29-34.
[33] Yao Q, Xu H, Zhang QQ, Zhou H and Qu LH. MicroRNA-21 promotes cell proliferation and down-regulates the expression of programmed cell death 4 (PDCD4) in HeLa cervical carcinoma cells. Biochem Biophys Res Commun 2009; 388: 539-542.
[34] Pennelli G, Galuppini F, Barollo S, Cavedon E, Bertazza L, Fassan M, Guzzardo V, Pelizzo MR, Rugge M and Mian C. The PDCD4/miR-21 pathway in medullary thyroid carcinoma. Hum Pathol 2015; 46: 50-57.
[35] Zhong X, Chung AC, Chen HY, Dong Y, Meng XM, Li R, Yang W, Hou FF and Lan HY. miR-21 is a key therapeutic target for renal injury in a mouse model of type 2 diabetes. Diabetologia 2013; 56: 663-674.
[36] Wang JY, Gao YB, Zhang N, Zou DW, Wang P, Zhu ZY, Li JY, Zhou SN, Wang SC, Wang YY and Yang JK. miR-21 overexpression enhances TGF-beta1-induced epithelial-to-mesenchymal

transition by target smad7 and aggravates renal damage in diabetic nephropathy. Mol Cell Endocrinol 2014; 392: 163-172.

[37] Matsuhashi S, Hamajima H, Xia J, Zhang H, Mizuta T, Anzai K and Ozaki I. Control of a tumor suppressor PDCD4: degradation mechanisms of the protein in hepatocellular carcinoma cells. Cell Signal 2014; 26: 603-610.

[38] Krug S, Huth J, Goke F, Buchholz M, Gress TM, Goke R and Lankat-Buttgereit B. Knock-down of Pdcd4 stimulates angiogenesis via up-regulation of angiopoietin-2. Biochim Biophys Acta 2012; 1823: 789-799.